



Contents lists available at ScienceDirect

## Journal of Hand Surgery Global Online

journal homepage: [www.JHSGO.org](http://www.JHSGO.org)

Original Research

## A Comparative Study of Porcine Small Intestine Submucosa and Cross-Linked Bovine Type I Collagen as a Nerve Conduit

Rasa Zhukauskas, MD, \* Debbie Neubauer Fischer, MS, \* Curt Deister, PhD, \*  
Nesreen Zoghoul Alsmadi, PhD, \* Deana Mercer, MD †

\* Axogen Corporation, Alachua, FL

† Department of Orthopaedics and Rehabilitation, University of New Mexico School of Medicine, Albuquerque, NM

## ARTICLE INFO

## Article history:

Received for publication March 1, 2021

Accepted in revised form June 22, 2021

Available online July 29, 2021

## Key words:

Biomaterial

Chronic Inflammation

Constructive remodeling

Nerve conduits

Nerve injury

**Purpose:** We compared 2 commercially available nerve conduits—the Axoguard Nerve Connector, made of porcine small intestine submucosa (SIS), and the NeuraGen Nerve Guide, made of cross-linked bovine type I collagen (Col)—using a rodent model at 4 weeks, specifically focusing on subchronic host responses to the implants.

**Methods:** A unilateral 5-mm sciatic nerve defect was created in 18 male Lewis rats and was repaired with SIS or Col conduits. After 4 weeks, histological evaluations of morphology, collagen content, macrophage polarization, vascularization, axonal regeneration, and myelination were conducted. To achieve a blinded examination, an independent qualified pathologist evaluated the images that were stained with hematoxylin-eosin,  $\alpha$ -smooth muscle actin, and Masson trichrome stains.

**Results:** The results showed a dominant macrophage type 2 (M2) response in the SIS group and a dominant macrophage type 1 (M1) response in the Col group. The SIS group showed deeper implant vascularization and fibroblast ingrowth than the Col group. Collagen deposition was higher within the lumen of the Col group than the SIS group. All Col conduits were surrounded by a colocalized staining of Masson trichrome and  $\alpha$ -smooth muscle actin, forming a capsule-like structure.

**Conclusion:** Distinctive histological features were identified for each conduit at the cellular level. The SIS conduits had a significantly higher number of host macrophages expressing M2 surface marker CD163, and the Col conduits showed a predominance of host macrophages expressing the M1 surface marker CD80. Data suggest that promoting the M2 response for tissue engineering and regenerative medicine is associated with a remodeling response. In addition, an independent analysis revealed an encapsulation-like appearance around all Col conduits, which is similar to what is seen in breast implant capsules.

**Clinical relevance:** The biomaterial choice for conduit material can play an important role in the host tissue response, with the potential to impact adverse events and patient outcomes.

Copyright © 2021, THE AUTHORS. Published by Elsevier Inc. on behalf of The American Society for Surgery of the Hand. This is an open access article under the CC BY-NC-ND license (<http://creativecommons.org/licenses/by-nc-nd/4.0/>).

Conduits used in peripheral nerve repair provide an off-the-shelf alternative to an autologous nerve graft for short-nerve gaps and prevent ischemia and poor functional outcomes resulting from direct repairs under tension.<sup>1</sup> The disadvantages of autologous nerve grafting are the limited supply of donor nerves, need for an

additional surgical site, potential complications at surgical sites, and potential size mismatches.<sup>2–5</sup> The United States has several commercially available nerve conduits made from porcine small intestine submucosa (SIS) or cross-linked bovine collagen type I (Col).<sup>6–8</sup>

The SIS is a processed extracellular matrix (ECM) scaffold that retains the features of native tissue. Extracellular matrix scaffolds are remodeled as they are replaced by infiltrating host cells through the deposition and assembly of a new, host-derived ECM matrix, which can be advantageous in regenerative medicine. Extracellular matrix scaffold-based biomaterials can be variable because of the biological nature of the source.<sup>9</sup> However, this process can typically

**Declaration of interests:** No benefits in any form have been received or will be received related directly or indirectly to the subject of this article.

**Corresponding author:** Deana Mercer, MD, Department of Orthopaedics and Rehabilitation, University of New Mexico School of Medicine, MSC10 5600 1, Albuquerque, NM 87106.

E-mail address: [dmercer@salud.unm.edu](mailto:dmercer@salud.unm.edu) (D. Mercer).

<https://doi.org/10.1016/j.jhsg.2021.06.006>

2589-5141/Copyright © 2021, THE AUTHORS. Published by Elsevier Inc. on behalf of The American Society for Surgery of the Hand. This is an open access article under the CC BY-NC-ND license (<http://creativecommons.org/licenses/by-nc-nd/4.0/>).

be controlled during manufacturing.<sup>10</sup> Purified collagen is another biomaterial used in nerve conduits. The collagen in Col biomaterials is dehydrated and cross-linked with agents such as N,N'-carbonyldiimidazole, isocyanate, formaldehyde, or glutaraldehyde. Although cross-linking is advantageous for improving mechanical strength and controlling degradation rate, it is also associated with some disadvantages such as the potential for cytotoxicity, calcification, and foreign body response.<sup>11–17</sup>

Studies performed by Badylak et al<sup>18</sup> reported the effects of cross-linking SIS and showed that cross-linked SIS is associated with a proinflammatory macrophage type 1 (M1) response, long-term inflammation, and the formation of scar tissue. Non-cross-linked SIS was associated with a prorepair macrophage type 2 (M2) response with organized, site-appropriate tissue remodeling and an absence of persisting inflammation.<sup>18</sup> In addition, these studies showed that M1 produces proinflammatory cytokines, whereas M2 excretes immunomodulatory cytokines. Both types of macrophages are critical in the process of tissue repair.<sup>18</sup> The  $\alpha$ -smooth muscle actin ( $\alpha$ -SMA)-positive myofibroblasts cells are another key player during peripheral nerve repair. High expression of  $\alpha$ -SMA can be beneficial for wound contraction and closure; however, it may affect axonal growth and maturation and may contribute to neuropathic pain.<sup>19</sup>

In this study, we examine the tissue remodeling and host macrophage response of 2 conduits in a rodent model of sciatic nerve repair at 4 weeks after surgery. We hypothesize that the SIS would be more biocompatible than the Col.

## Materials and Methods

### Conduit materials

Two commercially available, US Food and Drug Administration-cleared (510[k]) medical device (nerve conduit) implants were used in this study. The Axoguard Nerve Connector is an acellular, non-cross-linked SIS used for the repair of peripheral nerve discontinuities. It is manufactured by Cook Biotech and is distributed by Axogen Corporation. NeuraGen Nerve Guide is a cross-linked bovine Col implant used for the repair of peripheral nerve discontinuities. It is manufactured by Integra LifeSciences Corporation. Both medical devices were implanted in accordance with their instructions for use.

### Surgical procedures

A total of 18 male Lewis rats (271–303 g; Envigo) underwent unilateral sciatic nerve transection with a 5-mm gap and conduit repair. The repairs were performed using the SIS nerve conduit ( $n = 9$ ) or the Col nerve conduit ( $n = 9$ ). The sample size was chosen based on prior similar experiments. Surgical procedures and animal care conformed to National Institutes of Health guidelines, and the use of laboratory animals was approved by the University of Florida Institutional Animal Care and Use Committee. As described by Badylak et al,<sup>18</sup> the switch between M1 and M2 occurs between 2 and 4 weeks, and the changes are less prominent after the 4-week mark; thus, the 4-week mark was chosen. The 5-mm gap is a noncritical gap. In the rat sciatic nerve model, axonal regeneration is expected at the 5-week mark, and a complete bridge of the gap is anticipated at this time period. The goal was to observe the host response remodeling of the implant material, which occurs by 28 days.<sup>9,20</sup> The  $\alpha$ -SMA-positive tissue deposition can be observed as early as 4 weeks. After 4 weeks, nerve tissues were explanted and processed for histological evaluation. Functional testing was not included because the time point was too short for meaningful recovery in a transection model.

### Histology

Transverse 5- $\mu$ m paraffin-embedded sections were collected at 5 levels (L1–L5): the proximal nerve stump within the conduit (L1), the nerve gap area (L2–L4), and the distal nerve stump within the conduit (L5). Hematoxylin-eosin and Masson trichrome (MT) staining were performed using standard methods. For immunohistochemistry, antibodies against neurofilament-heavy polypeptide (NF; 1:500), Myelin Basic Protein (MBP; 1:100),  $\alpha$ -SMA (1:1000), macrophages M2 (CD163; 1:100), macrophages M1 (CD80; 1:100), and phagocytic cells (CD68; 1:500; Abcam) were used. Gross evaluation included assessments for adhesions, local hematomas/seromas, and inflammation at the implant site. The degree of soft-tissue attachments (Table E1, available on the Journal's website at [www.jhsgo.org](http://www.jhsgo.org)) was scored as described previously.<sup>21</sup> In addition, an independent, blinded pathologist examined the slides stained with hematoxylin-eosin, MT, and  $\alpha$ -SMA.

M1 and M2 macrophage polarization and the M2:M1 ratio were determined using immunohistochemistry as described previously.<sup>18</sup> A qualitative analysis of the fibroblast/vasculature depth of ingrowth was performed using a scoring system described in Table E2 (available on the Journal's website at [www.jhsgo.org](http://www.jhsgo.org)).

Collagen deposition/fibrosis was evaluated using MT staining. An image analysis was performed using manual color thresholding and area measurement functions of ImageJ software (FIJI). Axonal regeneration and myelination were characterized using antibodies against NF and MBP, respectively. NF- and MBP-positive staining were quantified at 4 different levels of the nerve repair site: the proximal stump (L1) and 3 levels within the nerve gap (L2–L4). Data are presented as mean  $\pm$  standard deviation of the percentage area.

### Statistical analysis

The statistical analysis was performed using Minitab 18.1 (Minitab, Inc). For comparisons between 2 sets, the Mann-Whitney U test was used. For data sets with multiple comparisons, the Friedman test was used with the level blocked (eg, comparison between SIS and Col groups). If significant, post hoc testing was performed with Mann-Whitney U test using Hochberg step-up procedure for multiple comparisons correction. Statistical significance was set at a  $P$  value  $\leq .05$ .

## Results

During implantation, saturability was similar between the conduits. The SIS conduit is semitransparent when hydrated, which allowed for the visualization of nerve placement into the conduit during implantation. The Col conduits remain opaque, even with hydration.

Upon explant, the filmy, transparent, and avascular soft tissue surrounding both conduits and the sciatic nerves was separated using blunt dissection. The Col conduits retained their tubular form with well-defined edges, and the SIS conduits conformed to the size and shape of the nerves (Fig. 1). Within the Col conduit group, 2 of 9 animals had small hematomas and adhesions involving less than 25% of the device surface area at the distal coaptations (Fig. 1A, black arrow). Adhesion formation may be related to factors including suture irritation and the mobile implant edge. Hematoma formation around the distal coaptation area may be related to the fluid collection at the lowest point of the wound or a higher degree of irritation because of motion. Hematoma formation may also contribute to adhesion development. The residual conduit length was measured in situ. From the time of the implants (4 weeks), Col conduits increased in length by 3.89% and SIS conduits decreased

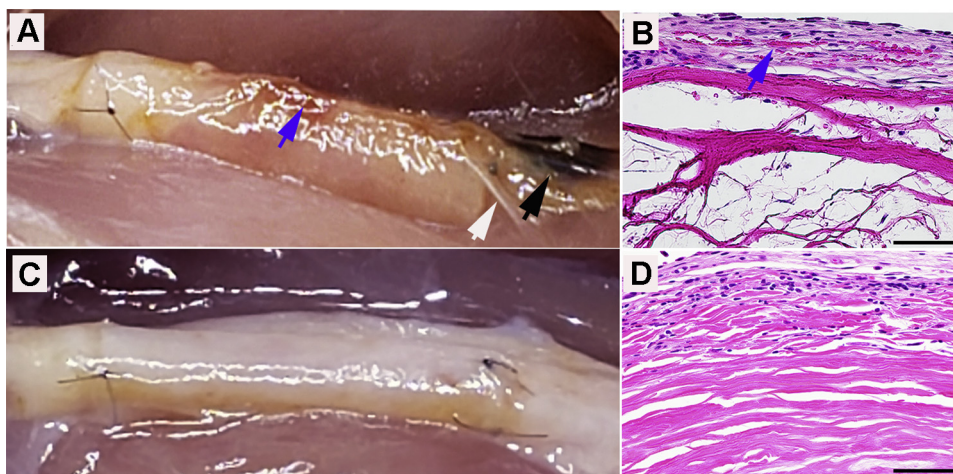


**Figure 1.** Representative images of repair with both **A** Col and **C** SIS conduits at 4 weeks. Small hematomas (black arrow), adhesion (white arrow), and **B** petechial hemorrhages (blue arrow) (magnification  $\times 400$ ; scale bars, 50  $\mu\text{m}$ ).

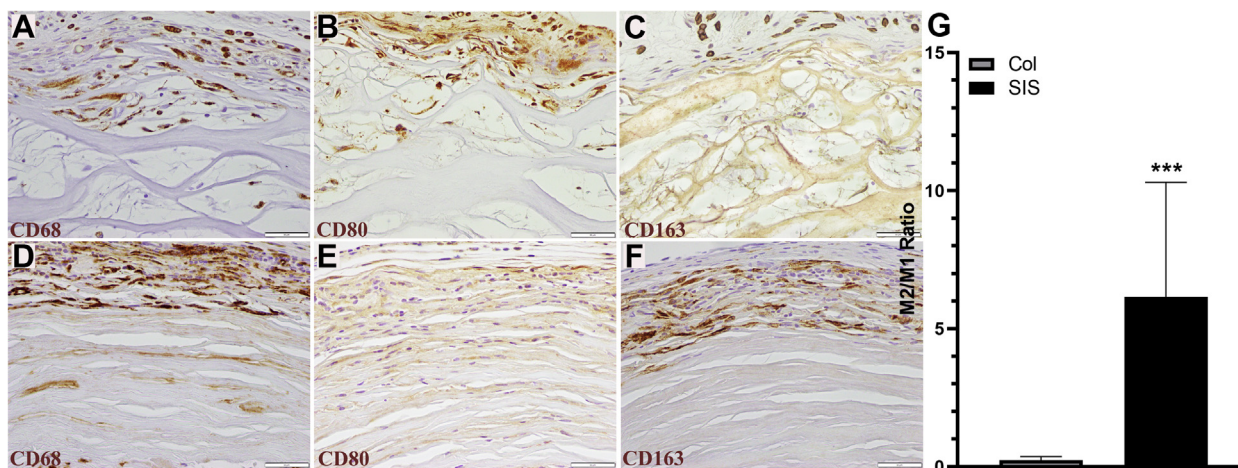


**Figure 2.** Representative photomicrographs of macrophages in the A–C Col repaired group and D–F SIS group. CD68 positive–stained cells represent both M1 and M2 phenotypes, fibroblasts, and endothelial cells. CD80 positive–stained cells represent the M1 (proinflammatory) phenotype, whereas CD163 positive–stained cells represent the M2 (anti-inflammatory) phenotype. G The M2/M1 ratios were different between the groups (immunohistochemistry stain; magnification  $\times 400$ ; scale bars, 50  $\mu\text{m}$ ).

by 6.67% on average. It has been observed that implants that have a time-controlled degradation profile tend to swell and increase in certain dimensions over several weeks after implantation until remodeling occurs. Cross-linked bovine collagen type I conduits did not have measurable remodeling at 4 weeks, whereas SIS conduits were involved in remodeling, with some areas being replaced by the host tissues. This observation has been described previously in studies from Badylak et al.<sup>18</sup> and Gilbert et al.<sup>20</sup>

There was a varying degree of petechial hemorrhaging on the surfaces of all Col conduit implants (Fig. 1A). A study by Shimizu et al.<sup>22</sup> showed that the friction between the walls of vessels and surrounding tissues could cause petechial hemorrhages. Microscopic evidence of petechial hemorrhages was also seen in the outer and inner layers of Col conduits indicated by erythrocyte infiltration (Fig. 1B). There were no petechial hemorrhages on the SIS implants (Fig. 1C). Gastrocnemius muscle atrophy was evident in the operated limbs of all animals. The wet muscle weight ratio (ie, operated limb muscle weight/nonoperated limb muscle weight) was  $0.33 \pm 0.2$  in both groups. Minimal recovery of gastrocnemius muscle weight was an expected finding given the early time point used in this study.

The pathology report revealed an overall higher number of macrophages and lymphocytes present in the sites with SIS conduits, which is thought to be related to the initiation of remodeling immediately after implantation. To better understand the host tissue response, immunohistochemical methods were used to determine the macrophage differentiation (Fig. 2). The Col conduit group was associated with a dominant M1 response (Fig. 2B), with  $10.77 \pm 2.71$  cells stained with CD80 (M1 marker; Fig. 2B) and  $2.57 \pm 1.27$  cells with CD163 (M2 marker; Fig. 2C) in  $100,000 \mu\text{m}^2$  of the device. The SIS conduit group was associated with a dominant M2 response (Fig. 2F), with  $26.00 \pm 8.16$  cells stained with CD163 and  $5.91 \pm 3.38$  cells with CD80 (Fig. 2E) in  $100,000 \mu\text{m}^2$  of the device. The M2:M1 ratios (Fig. 2G) of the SIS and Col conduit groups were  $6.15 \pm 3.01$  and  $0.23 \pm 0.10$ , respectively ( $P < .001$  using the Mann-Whitney U Test).

The process of tissue remodeling following implantation has been shown to be associated with a robust macrophage response beginning as early as 2 days after implantation and continuing for several months depending on the material and clinical application, according to Brown et al.<sup>15</sup> With non-cross-linked biomaterials like SIS, which is nonautologous to the host, higher numbers of

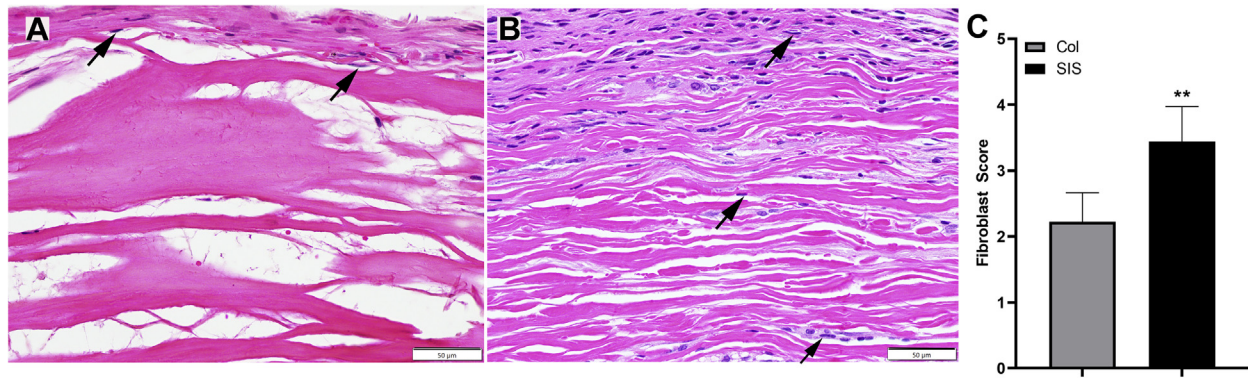


**Figure 3.** Representative photomicrographs showing fibroblast ingrowth in the 2 conduits: **A** the Col group and **B** the SIS group. **C** The depths of fibroblast ingrowth were different between groups (hematoxylin-eosin stain; magnification  $\times 400$ ; scale bars, 50  $\mu\text{m}$ ).

**Table**  
Mann-Whitney U Test Scores

Fibroblast Ingrowth Score Marker	Score = 0	Score = 1	Score = 2	Score = 3	Score = 4
Fibroblast ingrowth depth	Cells not present	Only at the interface	Peripheral	Localized deeper ingrowth	Consistent throughout the implant
Neovascularization depth	Not present	Only at the interface	Peripheral	Localized deeper ingrowth	Consistent throughout the implant

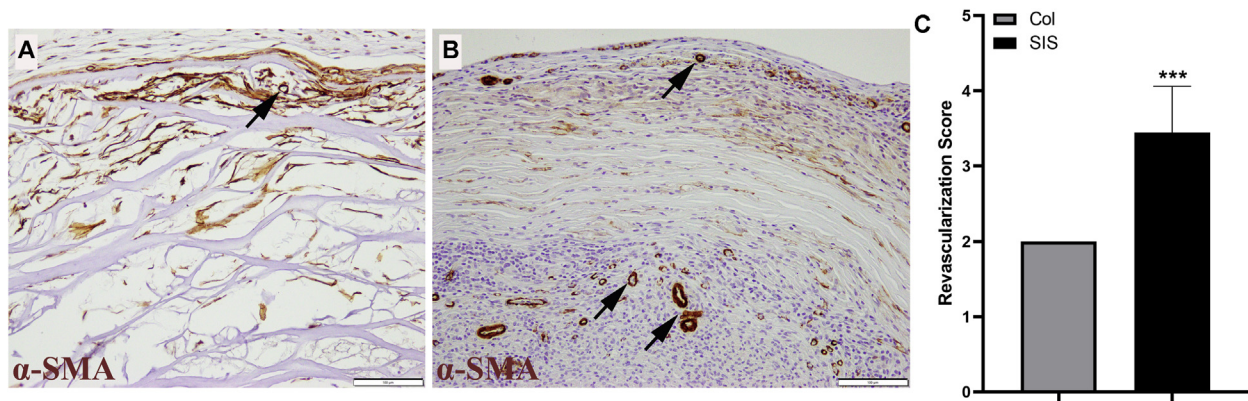


**Figure 4.** The  $\alpha$ -SMA-immunohistochemistry staining showing revascularization in both **A** the Col group and **B** the SIS group. **C** The revascularization scores were significantly different between groups ( $P < .001$  using the Wilcoxon signed rank test) ( $\alpha$ -SMA-immunohistochemistry stain; magnification  $\times 200$ ; scale bars, 100  $\mu\text{m}$ ).

mononuclear cells are expected due to cell access to the ECM. The phenotypic differentiation of these mononuclear cells differentiates between cytotoxic chronic inflammation and inflammation related to constructive remodeling. Clinical and nonclinical studies have demonstrated that the tissue cytokine and humoral response to SIS-ECM was consistent with a T helper 2 type of lymphocytic response and an M2 type of macrophage response; this resulted in complete remodeling of the implants with the resolution of the immune response over time. This observation was reported by Badylak et al<sup>18</sup> and Brown et al.<sup>15</sup>

The host fibroblast ingrowth depth in the conduits was evaluated qualitatively using cross-sections taken from the middle levels of the samples (L2–4) stained with hematoxylin-eosin (Fig. 3A, B). The fibroblast ingrowth score was calculated based on the fibroblast ingrowth depth and neovascularization depth (Table). The SIS conduit group (Fig. 3B) had an average score of  $3.44 \pm 0.53$ . The Col conduit group (Fig. 3A) had an average score of  $2.22 \pm 0.44$  (Fig. 3C;  $P = .002$  using the Mann-Whitney U test). In addition, the pathology report revealed signs of conduit remodeling in 7 of 9 SIS sites and 0 of 9 Col sites.

Vascularization was evaluated using  $\alpha$ -SMA staining (Fig. 4). Evidence of vascularization was seen in both conduits (Fig. 4B), with an average score of  $3.44 \pm 0.53$  for the SIS conduit group and that of  $2.00 \pm 0.00$  for the Col conduit group (Fig. 4A, C;  $P < .001$  using the Wilcoxon signed rank test). The Mann-Whitney U test could not be used on this data set because all the Col nerve conduit scores were 2.

Collagen deposition in the conduit lumen/regenerating nerve cable was evaluated using MT staining. A quantitative analysis exhibited an average score of  $18.85\% \pm 4.29\%$  for the Col group versus  $9.5\% \pm 1.65\%$  for the SIS group (Fig. 5;  $P < .001$  using the Mann-Whitney U test).

The  $\alpha$ -SMA staining was also used to detect the presence of myofibroblasts in peripheral nerve tissues.<sup>6</sup> Myofibroblasts are involved in the inflammatory response to injury.<sup>23</sup> They migrate to the injury site and produce cytokines that enhance the inflammatory response.<sup>24</sup> Figure 6 shows  $\alpha$ -SMA-positive staining in both conduits. Figure 6A1–3 shows a Col conduit, and Figure 6B1–3 shows an SIS conduit. Layers of myofibroblast cells (dark brown) were present around all Col conduits. A pathology analysis

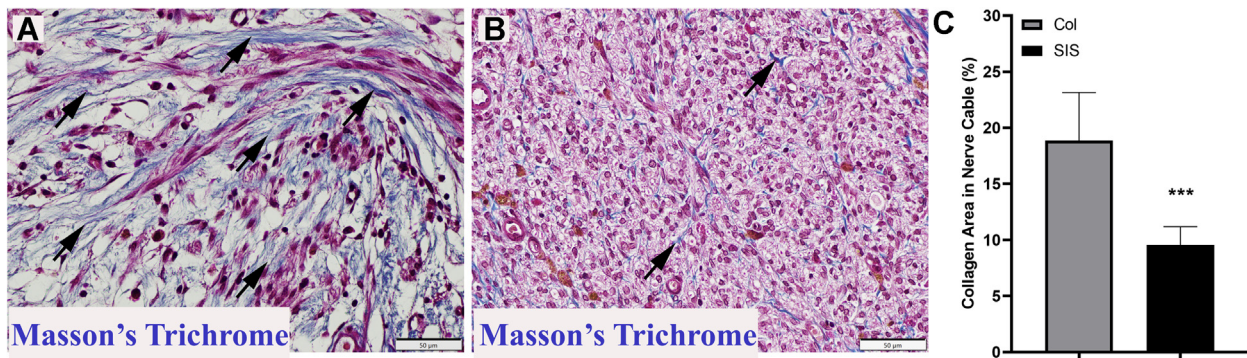


**Figure 5.** Histologic appearance of the regenerating nerve cable inside both A Col and B SIS conduits showing collagen fibers (blue). C The differences were significant between groups ( $P < .001$  using the Mann-Whitney U test) (MT stain; magnification,  $\times 400$ ; scale bars,  $50 \mu\text{m}$ ).

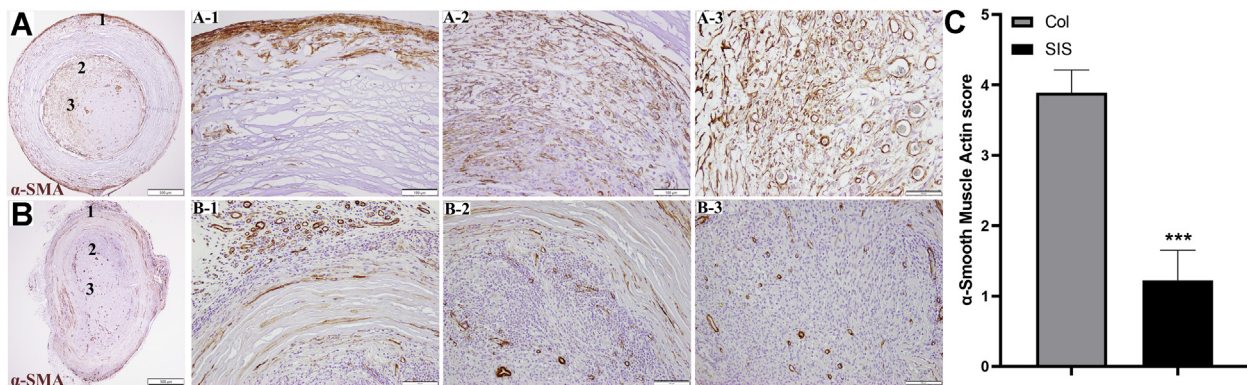


**Figure 6.** Representative photomicrographs of positive  $\alpha$ -SMA with the A1–A3 Col and B1–B3 SIS conduits. The numbers seen in panels A and B represent the levels depicted in A1–A3 and B1–B3, respectively ( $\alpha$ -SMA stain; magnification  $\times 200$ ; scale bars,  $100 \mu\text{m}$ ).

demonstrated colocalization of  $\alpha$ -SMA and MT staining, which is a sign of encapsulation similar to what has been reported in breast implant capsules.<sup>23</sup>

The NF staining density in the SIS conduit group at level 3 showed an average score of  $28.4\% \pm 3.4\%$  versus  $21.0\% \pm 4\%$  for the Col conduit group (Fig. 7). At level 4, the NF staining density was  $23.85\% \pm 8.14\%$  for the SIS conduit group (Fig. 7A, C) versus  $15.77\% \pm 5.02\%$  for the Col conduit group (Fig. 7B, C). The differences between the groups at both of these levels were significant (Fig. 7C; Friedman test,  $P < .001$ ; Mann-Whitney U test used post hoc, both levels'  $P$  values = .006 uncorrected). The MBP stain density was decreased in the distal levels of the repaired nerve compared with the more proximal levels in both groups (Fig. 7F). At level 3, the MBP stain density in the central region of the regenerating cables was  $18.14\% \pm 8.39\%$  for the SIS conduit group (Fig. 7E, F) versus  $10.36\% \pm 5.76\%$  for the Col conduit group (Fig. 7D, F). At level 4, the MBP stain density was  $11.62\% \pm 6.9\%$  in the SIS conduit group versus  $4.61\% \pm 43\%$  in the Col conduit group. Levels 3 and 4 were trending toward significance but were not significantly different (both  $P = .027$  with Mann-Whitney U post hoc). The threshold for 2 significant values with Hochberg step-up procedure is a  $P$  value of .025.

## Discussion

This study compared non-cross-linked SIS conduits with cross-linked collagen nerve conduits using a rodent model at 4 weeks, specifically focusing on the subchronic host responses to the implants. Gross evaluation under magnification showed a varying degree of petechial hemorrhages in the surrounding tissues of the

Col conduit group, confirmed by histopathology. The etiology of petechial hemorrhage formation is not clear; however, it has been reported that mild mechanical or chemical irritation may be the cause.<sup>22</sup> Friction between the vessel walls and the surrounding tissues can cause petechial hemorrhages to occur in the brain tissue, called "neurovascular friction."<sup>24</sup> Mild perivascular shear/irritation at the interface between Col implants and the surrounding tissues may have caused petechiae and punctate hematoma formation during normal animal movement. Further studies are necessary to understand this phenomenon.

This study showed that SIS conduits elicited a higher overall host macrophage response, with a significantly higher number of host macrophages expressing prorepair M2 surface markers. M2 polarized macrophages are known to scavenge debris; produce high levels of interleukin (IL) 10, tumor growth factor  $\beta$ , and arginase; and inhibit the release of proinflammatory cytokines.<sup>18,25</sup> They also promote angiogenesis and recruit cells involved in constructive tissue remodeling.<sup>18,26,27</sup> Our data showed a high M2:M1 ratio in the SIS conduit group at level 3, which was accompanied by deeper revascularization and host fibroblast ingrowth throughout the whole thickness of the conduit. Macrophage differentiating was performed mid implant to eliminate reactions to suturing or other non-implant related responses. The overall higher numbers of macrophages and lymphocytes present in the SIS conduit group are consistent with the initiation of remodeling immediately after implantation, whereas remodeling is largely absent in the Col group. The Col group showed a predominance of host macrophages expressing the M1 marker CD80. Proinflammatory M1 macrophage populations excrete large

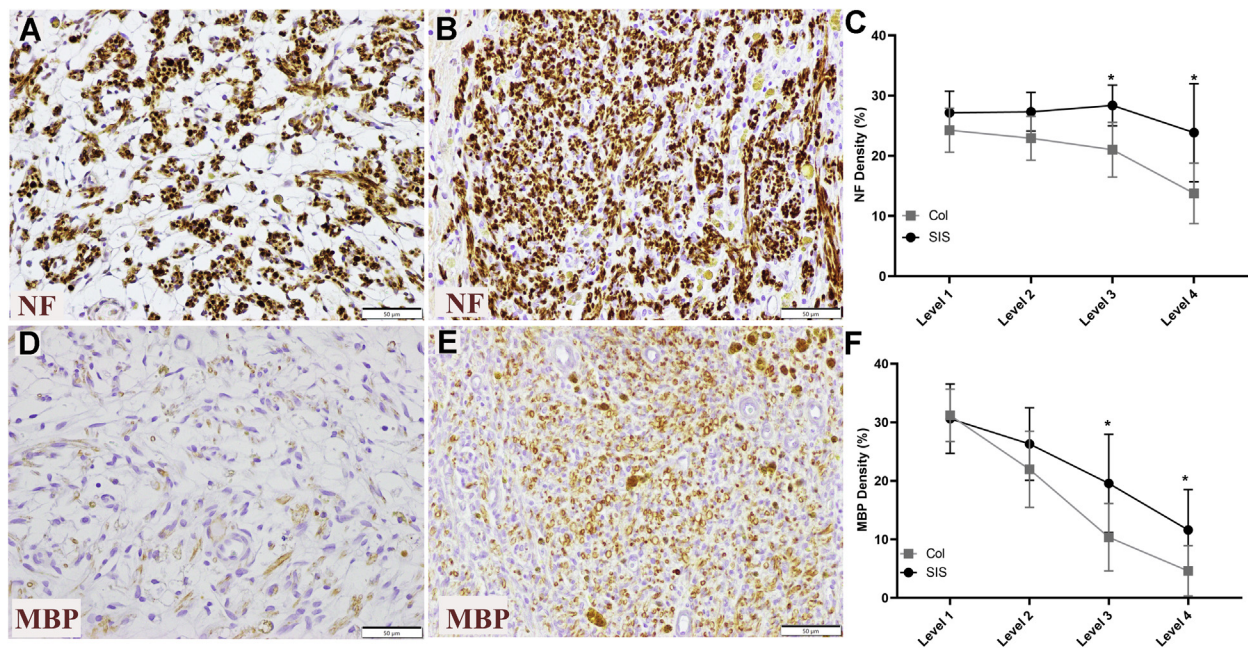


**Figure 7.** Representative images from level 4 of the axonal regeneration and myelination in repairs with the **A, D** Col and **B, E** SIS conduits (immunohistochemistry stain [NF and MBP]; magnification  $\times 400$ ; scale bars, 50  $\mu\text{m}$ ). The regenerating nerve cable density was significantly different between groups at level 3 and level 4 ( $P = .006$ ). **C** The NF staining density was significantly different at level 4 for the SIS conduit group compared to the Col conduit group. **D, F** The stain density in the central region of the regenerating cable was significantly different between groups at level 3 and level 4 ( $P = .027$ ) (MBP stain; magnification  $\times 400$ ; scale bars, 50  $\mu\text{m}$ ).

amounts of nitric oxide, other reactive oxygen intermediates, and copious amounts of proinflammatory cytokines such as IL-12, IL-6, and tumor necrosis factor  $\alpha$ .<sup>18,26</sup> These results were consistent with previous studies by Badylak et al<sup>18</sup> and Valentin et al<sup>28</sup> in which they demonstrated that the M2 response was associated with an organized, site-appropriate tissue remodeling outcome and an absence of persisting inflammation. Badylak et al<sup>18</sup> suggest that cross-linked scaffolds are associated with an M1 response, long-term inflammation, and the formation of scar tissue.

The most reliable marker of myofibroblastic cells is considered to be  $\alpha$ -SMA.<sup>29</sup> These cells are involved in the inflammatory response to injury, and they migrate to the site of injury, where they produce cytokines enhancing the inflammatory response.<sup>23</sup> Myofibroblasts are both morphologically and functionally different from fibroblasts. High extracellular tension is a crucial stimulus for fibroblasts to differentiate into proto-myofibroblasts.<sup>29</sup> As described by Tomasek et al,<sup>29</sup> myofibroblast differentiation depends both on the mechanical stress that develops within a given tissue and on the local expression of growth factors such as tumor growth factor  $\beta 1$ . As tension develops, the collagen fibers and the cells align parallel to the principal strain in the collagen lattice. The maintenance of the proto-myofibroblast phenotype requires continuous interaction between cell-generated stress and the reaction of a substratum that is sufficiently stiff to resist this force. Weng et al<sup>19</sup> and Wang et al<sup>30</sup> demonstrated that mechanical tension applied exogenously or generated endogenously can regulate  $\alpha$ -SMA expression. This generates contractile forces in nonmuscle cells, which upregulate the contractile activity of fibroblasts.<sup>19,31,32</sup> Weng et al<sup>19</sup> concluded that the biological characteristics of myofibroblasts ( $\alpha$ -SMA) may “entrap” regenerated nerve fibers and cause spontaneous pain. Baum and Duffy<sup>24</sup> demonstrated fibroblast differentiation into myofibroblasts in culture by the exogenous addition of inflammatory mediators found in the diseased heart, such as tumor growth factor  $\beta$  and IL-1 $\beta$ . This led to the hypothesis that the inflammatory response in the heart

may be a primary trigger for this phenotype switch.<sup>23</sup> Substrate rigidity can also directly activate macrophages and induce proinflammatory cytokine production.<sup>33</sup> The persistence of myofibroblasts within the tissue results in stiffening and deformation.<sup>34</sup> The myofibroblast’s internal microfilaments form a contractile mechanism with extracellular fibronectin. This contractile force is maintained over time and reinforced by the deposition of collagen.<sup>35</sup> Therefore, the increased expression of  $\alpha$ -SMA seen in the collagen conduit group may explain the higher level of collagen deposition seen in this group.

#### Clinical relevance

It is important to understand biocompatibility in implanted materials. The results of this study are in agreement with data from the literature published by Badylak<sup>9</sup> and Badylak et al,<sup>18</sup> indicating that cross-linking is associated with proinflammatory macrophages, long-term inflammation, and the formation of scar tissue.

#### Limitations

This study’s limitation was that there was no benchtop comparison to characterize stiffness, elasticity, or myofibroblastic differentiation in cell culture between the 2 materials. This study demonstrated that the biomaterial choice for conduit material can play an important role in the host tissue response, with the potential to impact adverse events and patient outcomes.

#### Acknowledgments

Axogen Corporation internally funded this work. The authors acknowledge the contribution of Dr Sharon Hook, a board-certified pathologist, for providing the pathology report and the interpretation of the hematoxylin-eosin, MT, and  $\alpha$ -SMA staining.

## References

- Carvalho CR, Oliveira JM, Reis RL. Modern trends for peripheral nerve repair and regeneration: beyond the hollow nerve guidance conduit. *Front Bioeng Biotechnol*. 2019;7:337.
- Hundepool CA, Bulstra LF, Kotsougiani D, et al. Comparable functional motor outcomes after repair of peripheral nerve injury with an elastase-processed allograft in a rat sciatic nerve model. *Microsurgery*. 2018;38(7):772–779.
- Bulstra LF, Hundepool CA, Friedrich PF, Bishop AT, Hovius SER, Shin AY. Functional outcome after reconstruction of a long nerve gap in rabbits using optimized decellularized nerve allografts. *Plast Reconstr Surg*. 2020;145(6):1442–1450.
- Bain JR. Peripheral nerve and neuromuscular allotransplantation: current status. *Microsurgery*. 2000;20(8):384–388.
- Brenner MJ, Hess JR, Myckatyn TM, Hayashi A, Hunter DA, Mackinnon SE. Repair of motor nerve gaps with sensory nerve inhibits regeneration in rats. *Laryngoscope*. 2006;116(9):1685–1692.
- Shin RH, Friedrich PF, Crum BA, Bishop AT, Shin AY. Treatment of a segmental nerve defect in the rat with use of bioabsorbable synthetic nerve conduits: a comparison of commercially available conduits. *J Bone Joint Surg Am*. 2009;91(9):2194–2204.
- Whitlock EL, Tuffaha SH, Luciano JP, et al. Processed allografts and type I collagen conduits for repair of peripheral nerve gaps. *Muscle Nerve*. 2009;39(6):787–799.
- Pabari A, Yang SY, Seifalian AM, Mosahebi A. Modern surgical management of peripheral nerve gap. *J Plast Reconstr Aesthet Surg*. 2010;63(12):1941–1948.
- Badylak SF. The extracellular matrix as a biologic scaffold material. *Biomaterials*. 2007;28(25):3587–3593.
- Hussey GS, Dziki JL, Badylak SF. Extracellular matrix-based materials for regenerative medicine. *Nat Rev Mater*. 2018;3(7):159–173.
- Gough JE, Scotchford CA, Downes S. Cytotoxicity of glutaraldehyde crosslinked collagen/poly(vinyl alcohol) films is by the mechanism of apoptosis. *J Biomed Mater Res*. 2002;61(1):121–130.
- van Wachem PB, Zeeman R, Dijkstra PJ, et al. Characterization and biocompatibility of epoxy-crosslinked dermal sheep collagens. *J Biomed Mater Res*. 1999;47(2):270–277.
- Levy RJ, Schoen FJ, Sherman FS, Nichols J, Hawley MA, Lund SA. Calcification of subcutaneously implanted type I collagen sponges. Effects of formaldehyde and glutaraldehyde pretreatments. *Am J Pathol*. 1986;122(1):71–82.
- Vasudev SC, Chandy T. Effect of alternative crosslinking techniques on the enzymatic degradation of bovine pericardium and their calcification. *J Biomed Mater Res*. 1997;35(3):357–369.
- Brown BN, Londono R, Tottey S, et al. Macrophage phenotype as a predictor of constructive remodeling following the implantation of biologically derived surgical mesh materials. *Acta Biomater*. 2012;8(3):978–987.
- Ye Q, Harmsen MC, van Luyn MJ, Bank RA. The relationship between collagen scaffold cross-linking agents and neutrophils in the foreign body reaction. *Biomaterials*. 2010;31(35):9192–9201.
- Delgado LM, Bayon Y, Pandit A, Zeugolis DI. To cross-link or not to cross-link? Cross-linking associated foreign body response of collagen-based devices. *Tissue Eng Part B Rev*. 2015;21(3):298–313.
- Badylak SF, Valentin JE, Ravindra AK, McCabe GP, Stewart-Akers AM. Macrophage phenotype as a determinant of biologic scaffold remodeling. *Tissue Eng Part A*. 2008;14(11):1835–1842.
- Weng W, Zhao B, Lin D, Gao W, Li Z, Yan H. Significance of alpha smooth muscle actin expression in traumatic painful neuromas: a pilot study in rats. *Sci Rep*. 2016;6:23828.
- Gilbert TW, Stewart-Akers AM, Simmons-Byrd A, Badylak SF. Degradation and remodeling of small intestinal submucosa in canine Achilles tendon repair. *J Bone Joint Surg Am*. 2007;89(3):621–630.
- Kokkalis ZT, Pu C, Small GA, Weiser RW, Venouziou AI, Sotereanos DG. Assessment of processed porcine extracellular matrix as a protective barrier in a rabbit nerve wrap model. *J Reconstr Microsurg*. 2011;27(1):19–28.
- Shimizu K, Nakamura N, Terao H. Mechanism of traumatic petechial hemorrhages in the brain–neurovascular friction. *J Neurosurg*. 1962;19:446–451.
- Kharbikar BN, Chendke GS, Desai TA. Modulating the foreign body response of implants for diabetes treatment. *Adv Drug Deliv Rev*. 2021;174:87–113.
- Baum J, Duffy HS. Fibroblasts and myofibroblasts: what are we talking about? *J Cardiovasc Pharmacol*. 2011;57(4):376–379.
- Bastos KRB, Alvarez JM, Marinho CR, Rizzo LV, Lima MR. Macrophages from IL-12p40-deficient mice have a bias toward the M2 activation profile. *J Leukoc Biol*. 2002;71(2):271–278.
- Mantovani A, Sica A, Sozzani S, Allavena P, Vecchi A, Locati M. The chemokine system in diverse forms of macrophage activation and polarization. *Trends Immunol*. 2004;25(12):677–686.
- Mantovani A, Sozzani S, Locati M, Allavena P, Sica A. Macrophage polarization: tumor-associated macrophages as a paradigm for polarized M2 mononuclear phagocytes. *Trends Immunol*. 2002;23(11):549–555.
- Valentin JE, Stewart-Akers AM, Gilbert TW, Badylak SF. Macrophage participation in the degradation and remodeling of extracellular matrix scaffolds. *Tissue Eng Part A*. 2009;15(7):1687–1694.
- Tomasek JJ, Gabbiani G, Hinz B, Chaponnier C, Brown RA. Myofibroblasts and mechano-regulation of connective tissue remodelling. *Nat Rev Mol Cell Biol*. 2002;3(5):349–363.
- Wang J, Zohar R, McCulloch CA. Multiple roles of  $\alpha$ -smooth muscle actin in mechanotransduction. *Exp Cell Res*. 2006;312(3):205–214.
- Desmoulière A, Chaponnier C, Gabbiani G. Tissue repair, contraction, and the myofibroblast. *Wound Repair Regen*. 2005;13(1):7–12.
- Serini G, Gabbiani G. Mechanisms of myofibroblast activity and phenotypic modulation. *Exp Cell Res*. 1999;250(2):273–283.
- Cheng Z, Shurer CR, Schmidt S, et al. The surface stress of biomedical silicones is a stimulant of cellular response. *Sci Adv*. 2020;6(15):eaay0076.
- Otranto M, Sarrazy V, Bonté F, Hinz B, Gabbiani G, Desmoulière A. The role of the myofibroblast in tumor stroma remodeling. *Cell Adh Migr*. 2012;6(3):203–219.
- Gabbiani G. The myofibroblast in wound healing and fibrocontractive diseases. *J Pathol*. 2003;200(4):500–503.